ERF
European Rotorcraft Forum

EVALUATION OF ROTOR BLADE MODELS FOR ROTOR OUTWASH

F. Rovere (2420587r@student.gla.ac.uk) , U. Morelli, (Umberto.morelli@glasgow.ac.uk), Rene Steijl (Rene.Steijl@glasgow.ac.uk) George N. Barakos (George.Barakos@glasgow.ac.uk)
CFD Laboratory School of Engineering, University of Glasgow, G12 8QQ, Scotland, UK

Luigi Vigevano (Luigi.Vigevano@polimi.it),
Department of Aerospace Science, Politecnico of Milan, 20156 MI, IT

Abstract
In this work Computational Fluid Dynamics is used as a tool for rotor outwash evaluation. The paper concentrates on the validation of the method, presents different modelling approaches and concludes with suggestions on the use of the method for detailed simulations of rotor outwash. The required computer resources for the detailed computations of the wake are also discussed.

1. INTRODUCTION

Rotorcraft outwash is the radial flow induced by a rotor wake when interacting with the ground with the aircraft operating in ground effect (IGE). This phenomenon is mainly affecting hovering rotorcraft, but it is also relevant during taxiing. Aerodynamically, the outwash flow field has time averaged characteristics similar to those of a wall jet [1]. Although, it is characterized by intense vorticity produced by the blade, mainly at the tip, and advected within the wake. The outwash plays an important role in the operation of helicopters IGE, affecting access to the cabin and influencing the surrounding environment. Consequently, a prediction of the outwash is necessary in several scenarios, from ground personnel safety to simulation of brownout. Of course, the accuracy level required depends on the objective of each simulation.

2. NUMERICAL METHOD

The Helicopter Multi-Block (HMB) [3, 4, 5] code is used as the CFD solver for the present work. It solves the Unsteady Reynolds Averaged Navier-Stokes (URANS) equations in integral form using the Arbitrary Lagrangian Eulerian (ALE) formulation for time-dependent domains, which may include moving boundaries. The Navier-Stokes equations are discretised using a cell-centred finite volume approach on a multi-block or hybrid structured/unstructured grids. To evaluate the convective fluxes, Osher [6] and Roe [7] approximate Riemann solvers are used in HMB, while the viscous terms are discretized using a second order central differencing spatial discretisation. The Monotone Upstream centred Schemes for Conservation Laws, which is referred to in the literature as the MUSCL approach and developed by Leer [8], is used to provide third order accuracy in space. The HMB solver uses the alternative form of the Albada limiter [8,9] being activated in regions where large gradients are encountered mainly due to shock waves, avoiding the non-physical spurious oscillations. An implicit dual time stepping method is employed to perform the temporal integration, where the solution is marching in pseudo-time iterations to achieve fast convergence, which is solved using a first-order backward difference. The linearised system of equations is solved using the Generalised Conjugate Gradient method with a Block Incomplete Lower-Upper (BILU) factorisation as a pre-conditioner [10]. To allow an easy sharing of the calculation load for parallel job, a multi-block structured meshes are used. Overset grid and sliding plane methods are available in HMB [4, 11] to allow the relative motion between different components. Both methods have been widely employed for isolated rotor blades, such as the UH-60A and S-76 by Dehaeze *et al.* [12] and Jimenez *et al.* [13], respectively, and complete helicopter configurations [4].

For the present work, an overset grid method is employed to explore its capabilities with tiltrotor configurations.

3. RESULTS AND DISCUSSION

In the present work, different rotor blades and ground models are evaluated for the prediction of rotor outwash to determine the level of accuracy of each model. The considered rotor models include: (i) uniform actuator disk, (ii) non-uniform actuator disk and (iii) full rotor model. The ground is modelled as a solid wall and also by using a mirror condition. The test cases simulated were experimentally investigated at the University of Maryland [2]. In this experiment a small two-bladed rotor was operated parallel to a ground plane at different heights. The loads on the blade were measured using a micro mass balance and the flow-field was measured with Particle Image Velocimetry (PIV).

Results were obtained for a rotor height of one radius using a steady uniform actuator disk model and a solid wall boundary condition at the ground. The computed flow-field is shown in Figures 1(a) and 1(b) show the IGE and OGE computational domains employed for this work. The main difference is the wall present at the lower surface of the IGE domain. This wall condition can be approximated either with a stick boundary condition or with a simple mirror-image condition that reduces the required resolution, and CPU time, but simplifies the interaction of the rotor wake with the ground.

The employed blade geometry and the associated CFD grids can be seen in Figure 2. The first cell normal to the blade was set to $1.9 \cdot 10^{-6}$ m ($1.0 \cdot 10^{-4}$ c) and $9.5 \cdot 10^{-6}$ m ($5.0 \cdot 10^{-4}$ c) for the chimera and matched grids, respectively, which assures y+ less than 1.0 everywhere on the blade for the employed Re. In the chord wise direction, between 164 mesh points were used, whereas in the spanwise direction 141 mesh points were used. The blunt blade edges were modelled using 82 mesh points. A C-H multi-block topology was used around the blade, combined with a background mesh using the chimera method. For all cases, the position of the far-field boundary was extended to 3R (above) and 6R (below and radial) from the rotor plane, which assures an independent solution with the boundary conditions employed. The rotor hub was modelled as a cylinder, extending from inflow to outflow with a radius corresponding to 2.75% of the rotor radius R. A cylindrical mesh with uniform spacing of 0.5625° in the azimuthal direction is used as background. In the radial and vertical directions, a non-uniform spacing is used to have a finer mesh close to the wake region with a cell spacing of 0.05c, and coarser mesh towards the external boundaries. The same two-bladed rotor was used for IGE and OGE cases. For IGE, it was positioned over a flat ground plane at different heights. The rotor was set parallel to the ground plane and operated at a rotational frequency of 50 Hz which corresponds to a tip speed of 27.02 ms^{-1}. Table 1 lists the blade properties as presented in [2]. Table 2 presents the details of the employed grids. Since this is a model-scale rotor, the corresponding Reynolds number is very low, and this promotes flow separation. Figure 3 shows this clearly with friction lines on the rotor surface and with flow visualisation at a cross-section of the computational domain. The flow separation as a result of the highly cambered blade is visible. Figure 4 shows the differences in flow topology between the IGE and OGE computations using Q criterion. For the OGE, the employed mesh allowed for the wake to be resolved for about 1.5 rotor revolutions and it shows the well-established contraction downstream the rotor disk plane. For the OGE case the wake contracts but rapidly expands outwards generating a strong out-wash field. This outwash was measured during experiments and is compared in Figure 5 with the simulations. Figure 6 shows the time averaged outflow velocity profiles at different radial distances from the rotor. In the figures, the velocity field is normalized by the hover induced velocity (v_h). It is shown that the height of the wall jet is accurately predicted with this model, but the outflow velocity magnitude is somehow overestimated.

4. SUMMARY AND CONCLUSIONS

This paper presented simulation results for rotor outwash. The employed CFD method is an expensive tool if rough, order of magnitude computations are needed for operational analysis of helicopters. On the other hand, the detailed flow-field simulation allows for the identification of wake features, like regions of low outwash, that may be used to improve access to the helicopter IGE. The employed method is generic and can be used for the simulation of different aircraft configurations with no further adaption. In terms of the selected simulation methods, the use of actuator disks to represent the rotor blades was found to be the easiest and more robust method to use. Nevertheless, adding the effect of the rotor blades by modelling each individual one revealed a more detailed wake structure and showed to a greater detail the spatial development of the helicopter wake. This work is now directed towards simulation of dust, rain or show within the outwash of the helicopter.

5. NOTATION

c   chord of the blade

C_f Surface friction coefficient

M_{tip} Mach number at blade tip

N_b Number of blades

Re_{tip} Reynolds at blade tip

R   Radius of the blade

R/c   Camber to chord aspect ratio

V_h Hover induced velocity

z   Distance of the rotor from the ground plane

Ө   Linear twist angle

6. REFERENCES

[1] Glauert, M., "The wall jet," Journal of Fluid Mechanics, Vol. 1, No. 6, 1956, pp. 625–643.

[2] Lee, T. E., Leishman, J. G., and Ramasamy, M., "Fluid dynamics of interacting blade tip vortices with a ground plane," Journal of the American Helicopter Society, Vol. 55, No. 2, 2010, pp. 22005–22005.

[3] Lawson, S. J., Steijl, R., Woodgate, M., and Barakos, G. N., "High performance computing for challenging problems in computational fluid dynamics," Progress in Aerospace Sciences, Vol. 52, No. 1, 2012, pp. 19–29, DOI: 10.1016/j.paerosci.2012.03.004.

[4] Steijl, R. and Barakos, G. N., "Sliding mesh algorithm for CFD analysis of helicopter rotor-fuselage aerodynamics," International Journal for Numerical Methods in Fluids, Vol. 58, No. 5, 2008, pp. 527–549, DOI:10.1002/d.1757.

[5] Steijl, R., Barakos, G. N., and Badcock, K., "A framework for CFD analysis of helicopter rotors in hover and forward flight," International Journal for Numerical Methods in Fluids, Vol. 51, No. 8, 2006, pp. 819–847, DOI:10.1002/d.1086.

[6] Osher, S. and Chakravarthy, S., "Upwind schemes and boundary conditions with applications to Euler equations in general geometries," Journal of Computational Physics, Vol. 50, No. 3, 1983, pp. 447–481, DOI: 10.1016/0021-9991(83)90106-7.

[7] Roe, P. L., "Approximate Riemann Solvers, Parameter Vectors, and Difference Schemes," Journal of Computational Physics, Vol. 43, No. 2, 1981, pp. 357–372, DOI: 10.1016/0021-9991(81)90128-5.

[8] van Leer, B., "Towards the ultimate conservative difference scheme. V.A second order sequel to Godunov's Method," Journal of Computational Physics, Vol. 32, No. 1, 1979, pp. 101–136, DOI: 10.1016/0021-9991(79)90145-1.

[9] van Albada, G. D., van Leer, B., and Roberts, W. W., "A Comparative Study of Computational Methods in Cosmic Gas Dynamics," Astronomy and Astrophysics, Vol. 108, No. 1, 1982, pp. 76–84.

[10] Axelsson, O., Iterative Solution Methods, Cambridge University Press: Cambridge, MA, 1994.

[11] Jarkowski, M., Woodgate, M., Barakos, G. N., and Rokicki, J., "Towards consistent hybrid overset mesh methods for rotorcraft CFD," International Journal for Numerical Methods in Fluids, Vol. 74, No. 8, 2014, pp. 543–576, DOI: 10.1002/fld.3861.

[12] Dehaeze, F. and Barakos, G. N., "Aeroelastic CFD Computations for Rotor Flows," Proceedings of the 37th European Rotorcraft Forum, ERF, Galarate, Italy, 2011, pp. 1–20. [29] Jimenez, A. and Barakos, G. N., "Hover Predictions on the S-76 Rotor using HMB2," Proceedings of the 53rd Aerospace Sciences Meeting, AIAA, Kissimmee, Florida, 2015, pp. 1–34.

[13] Jimenéz Garcia, A. and Barakos, G.N. (2018) Accurate predictions of rotor hover performance at low and high disc loadings. Journal of Aircraft, 55(1), pp. 89-110. (doi:10.2514/1.C034144)
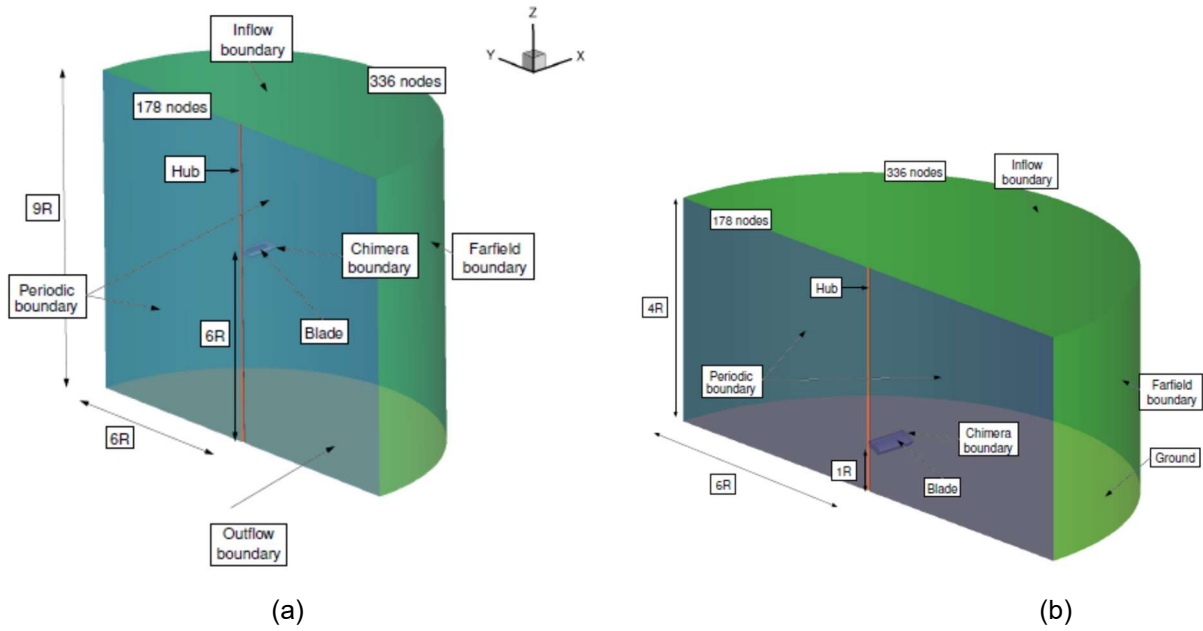
Figure 1: (a) OGE and (b) IGE computational domains and boundary conditions used for numerical simulations.
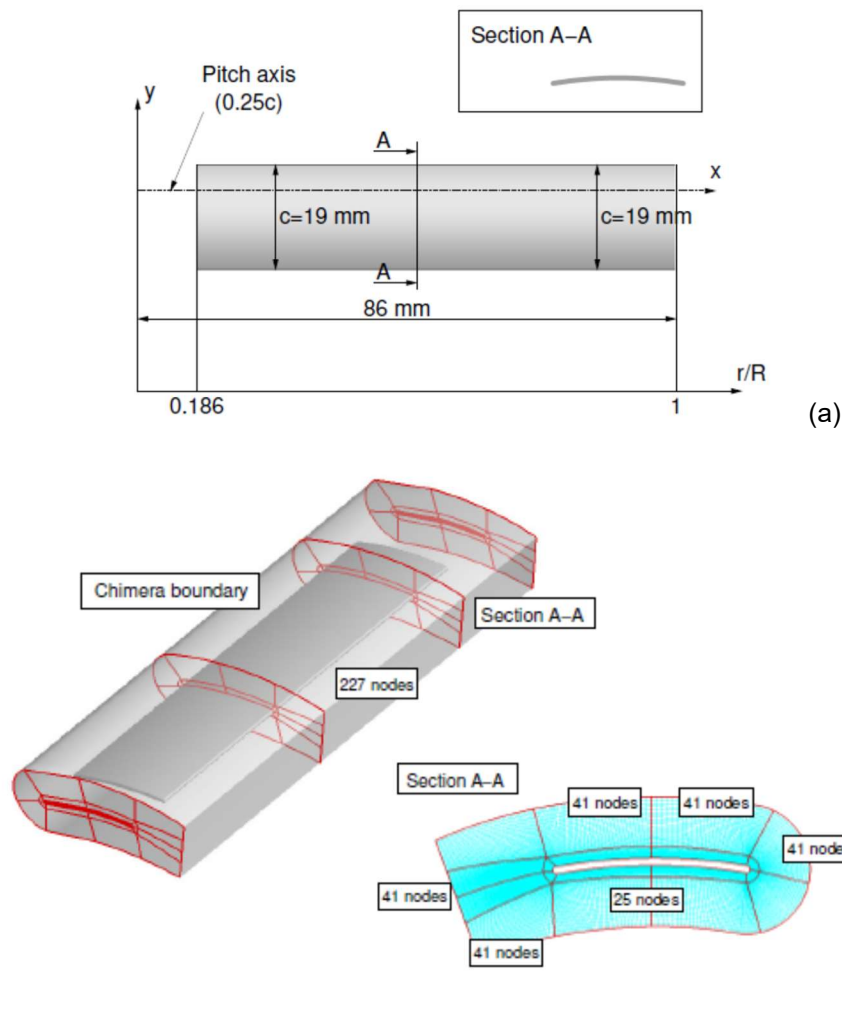

Figure 2: (a) Geometry of the model-scale blade. (b) Detailed view of the blade surface showing the Chimera method boundary and the distributions of the CFD grid points around the blade.

Table 1: Geometry of the employed rotor [2].

Parameter	Value
Number of blades, N_b	2
Rotor radius, R	86 mm
Blade chord (constant), c	19 mm
Aspect ratio, R/c	3.7
Camber to chord ratio	0.0645
Linear twist angle, Ө	0°

Table 2: Properties of the employed CFD grids.

Grid	Type	Background mesh size	Foreground mesh size	Overall mesh size	Variation mesh size	Wall distance
I	Chimera	9.5 M	6.6 M	16.0 M	12.5%	$1.0 \cdot 10^{-5}c$
II	Chimera	0.8 M	1.2 M	2 M	100%	$2.1 \cdot 10^{-5}c$

M= Million cells
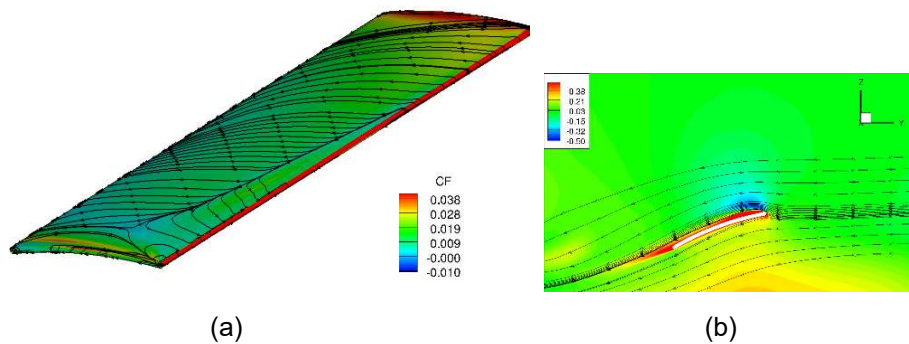

(a)   (b)

Figure 3: (a) surface friction and (b) Cp field around a blade section at 70%R.
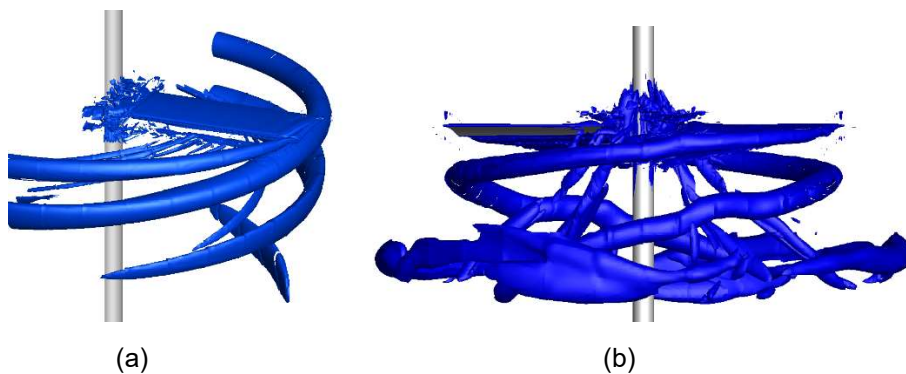

(a)   (b)

Figure 4: Wake visualization for the OGE (a) and IGE (b) cases.

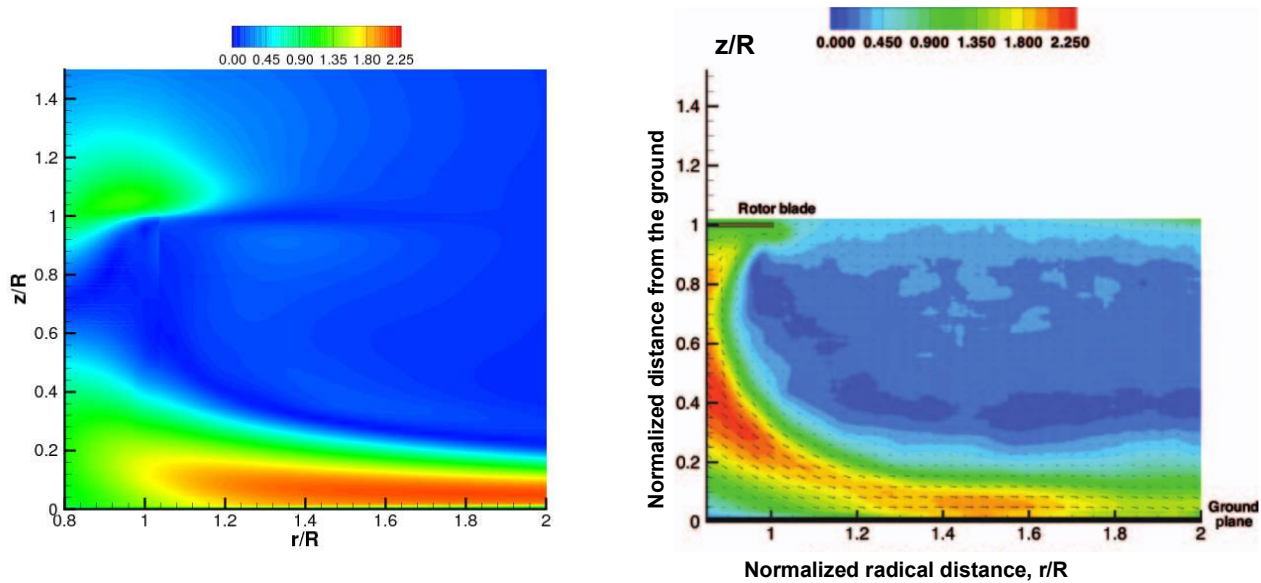(a) Computation, uniform actuator disk   (b) Experimental

Figure 5: Computed (left) and PIV [2] (right) results of the time-averaged velocity field normalized by the hover induced velocity through a radial plane at the ground plane for a rotor height of *z/R* = 1.0.
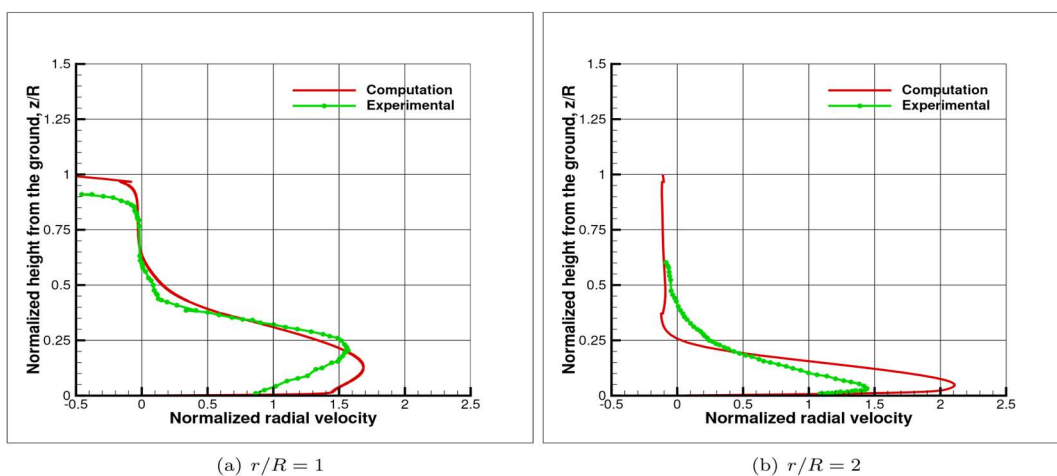

(a) $r/R = 1$

(b) $r/R = 2$

Figure 6: Computed and measured, time-averaged, velocity profiles at two radial distances away from the rotor. The rotor is operated at *z/R* = 1, Re_{tip} = 35,000 and M_{tip} = 0.08.